COMMUNICATION

# Thermomechanical and Thermal Contact Characteristics of Bismuth Telluride Films Electrodeposited on Carbon Nanotube Arrays

By *Himanshu Mishra, Baratunde A. Cola, Vijay Rawat, Placidus B. Amama, Kalapi G. Biswas, Xianfan Xu, Timothy S. Fisher,* and *Timothy D. Sands**

A miniaturized thermoelectric (TE) cooler module is composed of a large number of TE legs connected electrically in series and thermally in parallel.[1] TE devices operating near room temperature typically create a temperature difference of 30–50 °C, and the TE film thickness for such devices ranges from 10 to 100 μm.[2] From manufacturing and reliability perspectives, the design of TE cooler modules is often constrained by the shear stresses that result from differential thermal expansion, both during steady-state operation and during on/off cycling. In bulk systems, various strategies, such as spring-loaded systems, tension bolts, and welding, have been proposed to enhance compliance during device operation.[3] However, none of these strategies can be directly applied to thin-film based miniaturized TE devices. Additionally, for TE devices operating at higher temperatures, a pressing need exists for stable, compliant, and low thermal resistance interface materials between the TE element and the metallic interconnects. With this motivation, we report here a scalable electrodeposition process to integrate thick-film TE materials with carbon nanotubes (CNT) arrays.

Recently, CNT arrays have been reported to exhibit excellent fatigue strength under cyclic compressive loading[4] and as interface materials, they have been shown to achieve low thermal[5] and electrical[6] interface resistances at moderate contact pressures. Further, CNTs are amenable to heterogeneous integration with other materials.[7] These attributes suggest that compliant CNT arrays can be integrated with minimal parasitic additions to the total electrical and thermal resistances of a TE device.

[*] Prof. T. D. Sands, V. Rawat, P. B. Amama, K. G. Biswas
School of Materials Engineering, Purdue University West Lafayette IN 47907 (USA)
E-mail: tsands@purdue.edu
Prof. T. D. Sands, H. Mishra, B. A. Cola, V. Rawat, P. B. Amama, K. G. Biswas, X. Xu, Prof. T. S. Fisher
Birck Nanotechnology Center 1205 West State Street, West Lafayette, IN 49707-2057 (USA)
Prof. T. D. Sands
School of Electrical and Computer Engineering, Purdue University West Lafayette, IN 47907 (USA)
H. Mishra, B. A. Cola, Prof. T. S. Fisher
School of Mechanical Engingeering, Purdue University West Lafayette IN 47907 (USA)

DOI: 10.1002/adma.200803705

The common substrate for this work was $5 \times 6\,mm^2$ Ni(200 nm)/Ti (800 m)/$SiO_2$(1 μm)/Si(300 μm). For CNT array synthesis, some of these substrates were coated with a metal tri-layer structure of Fe (2.5 nm)/Al(10 nm)/Ti(30 nm) by electron-beam evaporation. Multi-walled CNT arrays were synthesized on these substrates by microwave-plasma chemical vapor deposition (MPCVD). The feed gases for the reaction were methane at 10 standard cubic centimeter per minute (sccm), and hydrogen at 50 sccm, The reaction temperature and pressure were 1173 K and 10 Torr (1 Torr = 133.32 Pa), respectively. Further details of the CNT synthesis by the MPCVD technique have been reported.[5] The remaining substrates, without CNTs, served as control samples. CNT arrays were imaged using a Hitachi S-4800 field-emission scanning electron microscope (FESEM) (Fig. 1). The average length and diameter of the CNTs were 25 μm and 40 nm, respectively.

Bismuth telluride ($Bi_2Te_3$) was chosen as a representative TE material for TE/CNT integration by electrodeposition, as it is the parent compound of the alloys used in commercial Peltier devices optimized for cooling at temperatures near 300 K.[8] Using a Bio-Analytical Systems (BAS) Epsilon Electrochemical System, $Bi_2Te_3$ was electrodeposited potentiostatically on the CNT array-coated substrates, and these films were compared with $Bi_2Te_3$ films electrodeposited directly on bare metallized substrates. A three-electrode setup was used with a CNT array-coated working electrode, platinum mesh counter electrode, and an Ag/AgCl (3 M NaCl, 0.175 V versus NHE) reference electrode. The deposition bath was composed of $Bi^{3+}$ ($0.75 \times 10^{-2}$ M) and $HTeO_2^+$ ($1 \times 10^{-2}$ M) (both Alfa Aesar, 99.999% pure) and $HNO_3$ (1 M) at 298 K.[2,9] Continuous one-minute pulses at −50 mV were applied between the working and the reference electrodes for about 10 h for electrodeposition

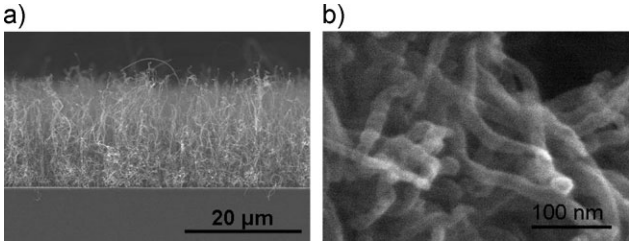


**Figure 1.** a) Side view of the MWCNT array and b) magnified image of MWCNT array.

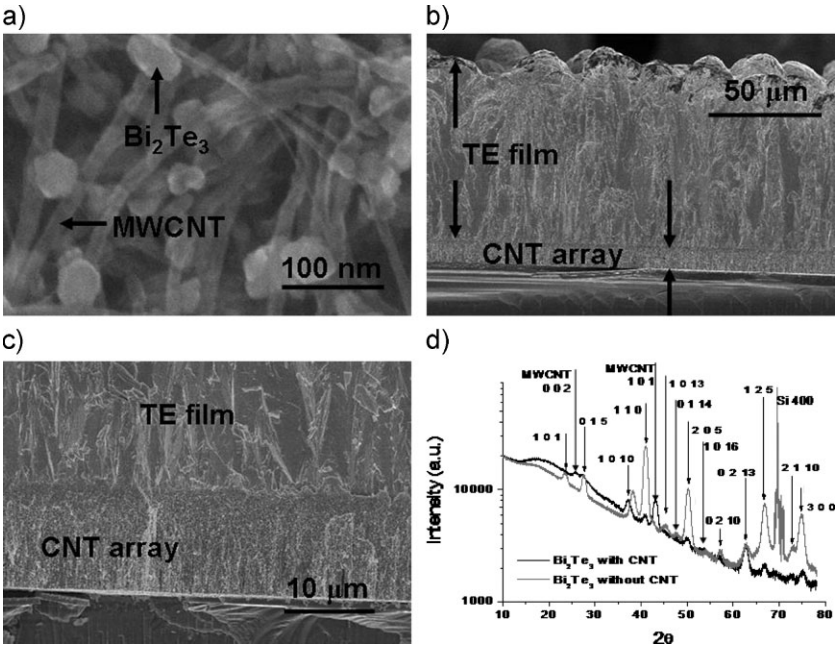


**Figure 2.** FESEM images showing a) nucleation of $Bi_2Te_3$ on individual MWCNTs, b) $Bi_2Te_3$ film/CNT array interface, and a c) magnified view of the $Bi_2Te_3$ film/CNT array interface. d) Comparison of X-ray diffraction pattern obtained from $Bi_2Te_3$ film electrodeposited on Ni(200 nm)/Ti(800 nm)/$SiO_2$(1 μm)/Si(300 μm) substrate and similar $Bi_2Te_3$ film electrodeposited on top of CNT arrays. The background in the samples is due to the relatively small size of the samples. All of the indexed diffraction peaks correspond to $Bi_2Te_3$ except MWCNT 002, MWCNT 101, and Si 400 peaks, labeled accordingly.

of ~50 μm thick $Bi_2Te_3$ films while maintaining a current density of about 5 mA $cm^{-2}$.

FESEM images were obtained to assess the morphology of the deposited TE/CNT heterostructures in both plan and cross-sectional views (Fig. 2a–c). It can be inferred from the FESEM images that the $Bi_2Te_3$ electrodeposited on and around the CNTs and ultimately extended above the CNT array as a continuous polycrystalline thin film. Different durations of electrodeposition resulted in film thicknesses ranging from 1 to 100 μm. Figure 2d shows X-ray diffraction patterns obtained from a $Bi_2Te_3$ film deposited directly on a silicon substrate and another grown on CNT array. The X-ray diffraction patterns confirm the presence of polycrystalline $Bi_2Te_3$ film on the CNT array, and the crystalline quality of the film is similar to that grown under similar electrodeposition conditions directly on a metalized silicon substrate. There is a detectable influence of the CNT array on the orientation of the $Bi_2Te_3$ film and that effect is observed in X-ray diffraction patterns. Some of the X-ray diffraction peaks observed in the pattern from the TE/M heterostructure were found to be missing, or slightly displaced in the pattern from the TE/CNT/M heterostructure (Fig. 2d). This is expected because the CNT array underlayer, as opposed to the metal substrate, is a non-planar substrate that is mechanically compliant. Thus, any influence of the substrate on crystallographic texture or deposition-induced stress will be manifested in subtle differences in peak intensity and diffraction angle. The possibility that carbon contamination from the CNTs could have influenced the texture and lattice parameters is remote, as there was no evidence of CNT dissolution during electrodeposition, and the $Bi_2Te_3$ were sufficiently thick to ensure that much of the growth occurred by $Bi_2Te_3$ deposition on $Bi_2Te_3$ rather than on CNTs directly.

For electrodeposition of $Bi_2Te_3$ patterns on CNT coated surfaces, towards development of a multi-coupled TE device, an optical lithography-based fabrication process was developed. On a CNT array coated surface (CNT/Ni (200 nm)/Ti (800 nm)/$SiO_2$ (1 μm)/Si (300 μm)), MicroChemicals AZ-9260 was spin-coated to obtain a photoresist layer with a thickness of ~7 μm. The photoresist was then patterned using optical lithography to open windows for the electrodeposition of $Bi_2Te_3$ patterns. The underlying metallic layer beneath the CNT layer provided an electrically conducting path through the sample, and the non-conducting photoresist mold restricted electrodeposition of TE materials to the exposed CNT region. This strategy may be employed to develop p- and n-type TE legs on CNT array coated metallic surfaces for thermomechanically compliant multi-couple TE microdevices (Fig. 3a, b).

To study the effects of the CNT interface material on the relative thermomechanical robustness of the TE/CNT/M heterostructure, the temperature excursion required to induce catastrophic failure (i.e., delamination of the film) was assessed for samples with and without the CNT interface material. The samples were compared to $Bi_2Te_3$ films (5 μm thickness) with lateral dimensions of 5 mm by 6 mm deposited directly on either metallized (Ni(200 nm)/Ti(800 nm)/$SiO_2$(1 μm)/Si(300 μm)) substrates or 25 μm thick CNT arrays grown on the same metallized substrate. Samples of both types were subjected to the same thermal cycle (ramp = 600 °C $h^{-1}$, dwell = 1 h, quench to room temperature) in forming gas (5% $H_2$, 95% Ar) in a controlled environment furnace (Lindberg horizontal, three zone tube furnace).

After each thermal cycle, the films were visually analyzed for signs of cracks or peeling, and the observations are presented in Table 1. For samples without a CNT interlayer, TE films completely delaminated from the substrates for a temperature rise ($\Delta T = T_{Furnace} - T_{Room}$) greater than 200 K. However, for the

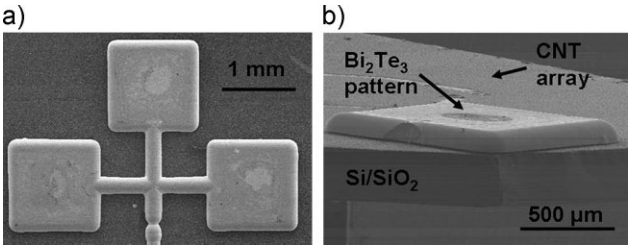


**Figure 3.** FESEM images showing a) top view of a $Bi_2Te_3$ pattern electrodeposited on top of a CNT array and b) side view of a thick $Bi_2Te_3$ pattern on CNT array.

**Table 1.** Thermomechanical failure of TE/CNT/Si and TE/Si structures.

| $\Delta T$ [K] | Maximum shear displacement [μm] | TE/Si structure observations | TE/CNT/Si structure observations |
|---|---|---|---|
| 50 | 3.12 | No effect | No effect |
| 100 | 6.24 | No effect | No effect |
| 150 | 9.36 | No effect | No effect |
| 200 | 12.48 | Film delaminated | No effect |
| 250 | 15.60 | Film delaminated | No effect |
| 300 | 18.72 | Film delaminated | No effect |
| 350 | 21.84 | Film delaminated | No effect |
| 400 | 24.96 | Film delaminated | Cracks appeared in film |

samples with CNT arrays as an interfacial layer between the $Bi_2Te_3$ film and the metallized substrate, the TE film remained well adhered to the substrate in all samples up to a temperature rise of 350 K (Table 1). Using the literature values for coefficients of thermal expansion for Si ($2.6 \times 10^{-6}\,K^{-1}$ [10]) and $Bi_2Te_3$ ($13.0 \times 10^{-6}\,K^{-1}$ [11]), the theoretical stress-free lateral displacement between the TE film and the substrate was calculated and is also indicated in Table 1. This maximum displacement was calculated at the perimeter of the $Bi_2Te_3$ film, assuming zero lateral displacement at the center. The maximum magnitude of the calculated stress-free displacement at the edge of the film with the CNT interface is 25 μm at the maximum temperature rise before failure. This value matches the average CNT length, supporting the hypothesis that the CNT interface exhibits high compliance up to the point that the CNTs are under tension. Once the CNTs are taut, further differential expansion induces mechanical failure manifested by cracking that initiates at the outer surface of the TE film under tension induced by buckling.

Effects on the thermal resistances between the metal and TE film, with and without a CNT layer, were measured as a function of interface temperature using a photoacoustic (PA) technique that has been detailed previously.[12,13] Briefly, in the PA technique, a sinusoidally modulated fiber laser is used to periodically heat the surface of the samples. The heated area of the sample's surface is surrounded by a sealed acoustic chamber; thus, a periodic pressure signal is produced, as measured by a microphone housed in the chamber wall. The measured pressure signal is used in conjunction with a thermal model to determine thermal interface resistance.[13]

In the PA technique, an 80 nm layer of Ti was deposited on relatively thin $Bi_2Te_3$ films (~30 μm) to absorb the laser energy at the sample surface and to ensure adequate sensitivity to interface resistance. The measured interface resistances for the $Bi_2Te_3$/CNT/M/Si and the $Bi_2Te_3$/M/Si (control) samples are illustrated as a function of interface temperature in Figure 4. The thermal interface resistance for the TE/CNT structures was found to be $30 \times 10^{-6}\,m^2\,K\,W^{-1}$, whereas for the TE/M contacts it was $\sim 2 \times 10^{-6}\,m^2\,K\,W^{-1}$ with an uncertainty of $\pm 1\,m^2\,K\,W^{-1}$. From a TE device-level perspective, the interface resistance should be less than 10% of the TE leg resistance. For $Bi_2Te_3$ films of 100 μm thickness, the measured thermal interface resistances of CNT-TE samples is ~55% of the intrinsic resistance of the TE film itself ($0.55\,K\,W^{-1}$, corresponding to a measured thermal conductivity of $1.8\,W\,(m\,K)^{-1}$ at 350 K). For all control samples the interface resistance was about 3% of the TE film thermal resistance

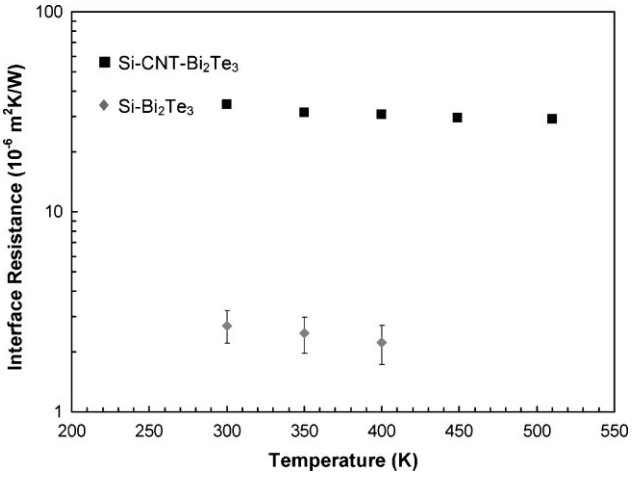


**Figure 4.** Thermal interface resistance as a function of interface temperature measured using the PA technique. The error in the interface resistance measurements is $\pm 1\,mm^2\,K\,W^{-1}$ and too small to appear on the log-scale for the larger resistance values.

($0.23\,K\,W^{-1}$, corresponding to a measured thermal conductivity of $1.5\,W\,(m\,K)^{-1}$ at 350 K). The higher thermal resistance at the TE/CNT/M/Si interface might be caused by reduction in the contact area due to the CNT array porosity. However, solid solutions of $Bi_2Te_3$ or other classes of TE materials with reduced thermal conductivity might still benefit from this strategy. For example, the thermal conductivity of a typical $(Bi_{0.7}Sb_{1.3})(Se_{2.91}Te_{0.09})$ alloy is $1.1\,W\,(m\,K)^{-1}$ at 330 K.[14] A 300 μm thick film of this TE material with the bulk value of thermal conductivity would present a thermal resistance that is about nine times larger than the interface resistance measured in the present study. Furthermore, prior work has shown that contact resistance decreases with increase in pressure on the contact.[5,6,12] Thus, mechanical compression of the TE/CNT contacts may reduce thermal contact resistance in the CNT-TE structures.

In conclusion, integration of CNT arrays and TE materials by an electrodeposition process has been shown to improve thermomechanical compliance of the contacts. The TE/CNT/M/Si hybrid contact with a maximum lateral dimension of 6 mm showed an increase of more than 150 K in the maximum temperature excursion without mechanical failure. Thermal interface resistances of the TE/CNT/M/Si and the TE/M/Si contacts to unalloyed $Bi_2Te_3$ films were measured, yielding $30 \times 10^{-6}$ and $2 \times 10^{-6}\,m^2\,K\,W^{-1}$, respectively. Although the CNT interface layer increases the total thermal interface resistance, the contribution of the CNT interfacial layer to the total thermal resistance is expected to be ~11% of the thermal resistance of $(Bi_{0.7},Sb_{1.3})(Se_{2.91},Te_{0.09})$ alloy TE leg of 300 μm thickness. Finally, a process flow was developed for patterned synthesis of TE films on CNT array coated surfaces.

## *Acknowledgements*

One of the authors (H. M.) thanks Ms. Patricia Metcalf for her help with the controlled environment furnace. Funding from the Cooling Technologies Research Center at Purdue University in support of this work is

gratefully acknowledged. Two of the authors (K. G. B and T. D. S) acknowledge funding from the Office of Naval Research (Award #N00014061641).

Received: December 16, 2008
Revised: February 10, 2009
Published online: June 24, 2009

[1] D. M. Rowe, C. M. Bhandari, *Modern Thermoelectrics*, Reston Publishing Company, Virginia **1983**.
[2] J. P. Fleurial, A. Borshchevsky, M. A. Ryan, W. M. Phillips, J. G. Snyder, T. Caillat, E. A. Kolawa, J. A. Herman, P. Mueller, M. Nicolet, *MRS Proc.* **1998**, *545*, 493.
[3] Y. Tanji, Y. Nakagawa, K. Kisara, M. Yasuoka, S. Moriya, T. Kumagai, M. Niino, R. Sato, 18th Int. Conf. Thermoelectric. Proc. **1999**, 260.
[4] P. V. Suhr, L. Ci, S. Sreekala, X. Zhang, O. Nalamasu, P. M. Ajayan, *Nat. Nanotechnol.* **2007**, *2*, 417.
[5] J. Xu, T. S. Fisher, *Int. J. Heat Mass Transfer* **2006**, *49*, 1658.
[6] M. Park, B. Cola, T. Siegmund, J. Xu, M. R. Maschmann, T. S. Fisher, H. M. Kim, *Nanotechnology* **2006**, *17*, 2294.
[7] A. D. Franklin, D. B. Janes, T. S. Fisher, T. D. Sands, *Appl. Phys. Lett.* **2008**, *92*, 013133-1-3.
[8] A. Ioffe, *Semiconductor Thermoelements and Thermoelectric Cooling*, Infosearch, London **1958**.
[9] M. S. Martin-Gonzalez, A. L. Prieto, R. Gronsky, T. D. Sands, A. M. Stacy, *J. Electrochem. Soc.* **2002**, *149*, C546.
[10] J. Schilz, L. Helmers, 16th Int. Conf. Thermoelectric. Proc. **1997**, 375.
[11] H. Watanabe, N. Yamada, M. Okaji, *Int. J. Thermophys.* **2004**, *25*, 221.
[12] B. A. Cola, Jun. Xu, C. Cheng, X. Xu, T. S. Fisher, *J. Appl. Phys.* **2007**, *101*, 054313-9.
[13] C. H. Hu, X. Wang, X. Xu, *J. Appl. Phys.* **1999**, *86*, 3953.
[14] M. V. Vedernikov, V. A. Kutasov, L. N. Luk'yanova, P. P. Konstantinov, 16th Int. Conf. Thermoelectric. Proc. **1997**, 56.